Magnetic field induced modification of superfluid density and interplane spectral weight in $YBa_2Cu_3O_y$

A. D. LaForge,[1,*] W. J. Padilla,[1,†] K. S. Burch,[1,‡] Z. Q. Li,[1] A. A. Schafgans,[1] Kouji Segawa,[2,3] Yoichi Ando,[3] and D. N. Basov[1]

[1]*Department of Physics, University of California, San Diego, La Jolla, California 92093, USA*

[2]*Central Research Institute of the Electric Power Industry, Komae, Tokyo 201-8511, Japan*

[3]*Institute of Scientific and Industrial Research, Osaka University, Ibaraki, Osaka 567-0047, Japan*

(Received 16 October 2008; revised manuscript received 28 January 2009; published 23 March 2009)

We report on the interlayer infrared response of $YBa_2Cu_3O_y$ in an applied magnetic field. This study explores both the underdoped (y=6.67 and 6.75) and optimally doped (y=6.95) regions of the phase diagram, and includes data for fields applied both parallel to the c axis and to the CuO_2 planes in this anisotropic superconductor. We focus on the transfer of optical conductivity spectral weight from high-frequency regions of the spectrum to the nondissipative superconducting condensate, and examine the effect of magnetic field upon this process. A sum-rule analysis reveals that magnetic fields $H \| c$ eliminate the high-frequency contribution to the superfluid density, returning the system to a more BCS-like energy scale. For fields $H \| CuO_2$, however, the high-energy contribution scales with the superfluid density, and the anomalous scheme of condensate formation is maintained, at least in underdoped y=6.67 and 6.75 samples. This behavior is discussed in relation to the change in electronic kinetic energy and shown to be closely related to the suppression of interplane phase coherence.

DOI: 10.1103/PhysRevB.79.104516 PACS number(s): 74.25.Gz, 74.25.Ha, 74.72.Bk

I. INTRODUCTION

Infrared spectroscopy is a powerful tool for studying condensed-matter systems. It provides numerous insights due to its sensitive resolution of subtle spectral characteristics, but also for its ability to utilize data from a wide frequency range to determine system properties based on conservation laws and sum rules. For example, one of the Kubo conductivity sum rules relates the integrated real part of the optical conductivity $\sigma_1(\omega)$, or spectral weight, over all bands to the number density N_e and mass m of electrons in the solid,[1]

$$\int_0^\infty d\omega \sigma_{1,\mathbf{r}}(\omega) = \frac{\pi}{2}\frac{ne^2}{m}. \tag{1}$$

If we restrict our attention to a single band, however, it is possible to relate the low-frequency spectral weight to the occupancy and dispersion of that band. In the tight-binding approximation the spectral weight is simply proportional to the electronic kinetic energy $K_\mathbf{r}$,[2–6]

$$\int_0^\Omega d\omega \sigma_{1,\mathbf{r}}(\omega) = \frac{\pi}{2}\frac{e^2 a_\mathbf{r}^2}{\hbar^2} K_\mathbf{r}. \tag{2}$$

A sum rule which is quintessential for the understanding of superconductivity was formulated by Ferrell, Glover, and Tinkham (FGT); it equates the spectral weight lost in the superconducting gap to the strength of the zero-frequency superconducting condensate, quantified by the superfluid density ρ_s,

$$\rho_{s,\mathbf{r}} = \int_{0^+}^\Omega d\omega [\sigma_{1,\mathbf{r}}^{\mathrm{N}}(\omega) - \sigma_{1,\mathbf{r}}^{\mathrm{SC}}(\omega)]. \tag{3}$$

The FGT sum rule[7] is valid for elemental superconductors which are well-described by the theory of Bardeen, Cooper, and Schreiffer (BCS). In this case the difference in spectral weight between the normal and superconducting states reaches the full value of ρ_s by an integration cutoff of only a few gap values. However, for many high-T_c cuprate superconductors, optical experiments[8–18] have revealed that the difference in conductivity only constitutes a portion of the superfluid when integrated up to several gap values. This behavior implies that the extra spectral weight in the superconducting condensate must be transferred from much higher energies, and also that the system experiences a lowering of electronic kinetic energy during the superconducting transition. The spectral weight shift during the transition is then described[4] by

$$\rho_{s,\mathbf{r}} = \int_{0^+}^\Omega d\omega [\sigma_{1,\mathbf{r}}^{\mathrm{N}}(\omega) - \sigma_{1,\mathbf{r}}^{\mathrm{SC}}(\omega)] + \Delta K_\mathbf{r}, \tag{4}$$

and is illustrated schematically in Fig. 1.

High-energy effects are common to at least four different families of cuprates, appearing in both ab-plane and c-axis measurements. Typically, they are only observed at doping levels below the optimal value, and not in the overdoped regime. Such broad occurrence and similarity in doping dependence prompted many to consider whether the lowering of electronic energy was an essential component to the superconducting mechanism in this class of materials. These questions sparked a need for experiments that could unambiguously identify the high-energy spectral weight transfer and access a weakened superconducting state to verify if the condensation scheme remained intact when the order parameter was suppressed. Infrared measurements in which the incident electric field is polarized parallel to the c axis are highly sensitive to changes in kinetic energy and therefore uniquely suited to address this experimental need. Further, the desired perturbation can be provided by application of an

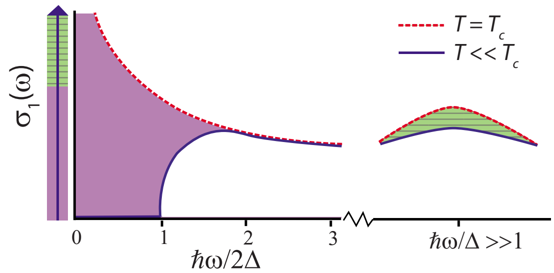

FIG. 1. (Color online) Optical conductivity of a superconductor in the normal (dashed lines) and superconducting (solid lines) states (schematic, adapted from Ref. 4). As the superconducting gap opens, spectral weight is shifted from finite frequencies to the δ function at zero frequency. In many cuprate superconductors the superfluid is composed of spectral weight transferred from both low- (solid shaded regions) and high- (horizontally hatched regions) frequency parts of the spectrum.

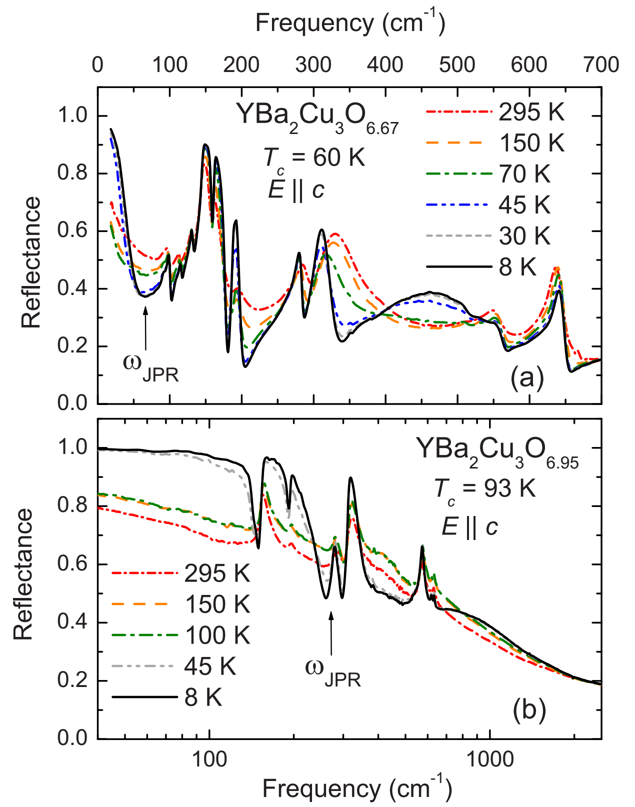

FIG. 2. (Color online) Infrared reflectance $R(\omega)$ of $YBa_2Cu_3O_y$ single crystals for dopings (a) $y=6.67$ and (b) 6.95 at several temperatures above and below T_c.

external magnetic field, which competes with superconductivity without promoting disorder. Consequently, the technique of infrared optics in magnetic field is an ideal tool for probing these phenomena.

We have previously reported on infrared measurements[19] of underdoped $YBa_2Cu_3O_y$, a prototypical high-T_c superconductor, recording the evolution of the spectral weight balance in magnetic field $H \| c$. We found that, from a sum rule--analysis point of view, the high-field data were less anomalous than at zero field. Here, we extend these results to include sum-rule analysis in magnetic field for data recorded at higher temperatures, as well as for magnetic fields oriented parallel to the CuO_2 planes. Section II provides details regarding our infrared magneto-optical experiment and reflectance data, and Sec. III presents the calculated optical conductivity. The sum-rule analysis of the conductivity data is described in Sec. IV and, lastly, connections to interlayer phase coherence and vortex lattice resonance modes are discussed in Sec. V.

II. INFRARED REFLECTANCE EXPERIMENT IN MAGNETIC FIELD

High-quality *ac*-face single crystals of $YBa_2Cu_3O_y$ (YBCO) were grown using a flux method[20] and annealed to achieve doping levels of $y=6.67$, 6.75 (both underdoped), and 6.95 (optimally doped). Transport measurements[21] reveal sharp transitions to the superconducting state at 60, 65, and 93 K, demonstrating the high purity of the crystals. For each doping several single crystals from a single batch were assembled to form mosaics approximately $3\times 6\ \mathrm{mm}^2$ in size.

Near-normal reflectance measurements were performed in a broadband Fourier transform spectrometer over a frequency range of 18–35 000 cm^{-1}. First, absolute reflectance was obtained at temperatures $T=8-295$ K by measuring sample reflectance relative to a stainless-steel reference mirror and normalizing by the reflectance of the sample coated with Au.[22] Then, changes in reflectance induced by magnetic field H were recorded via the ratio $R(T,H)/R(T,H=0)$ in a split-coil magnet[23] for field magnitudes up to 8 T. This step utilized an Al reference mirror to correct for minor spurious effects in the magnet system.

Reflectance spectra for the YBCO system (Fig. 2) are weakly metallic near room temperature, with an upturn toward $R=1$ as $\omega\to 0$. The sharp peaks in the far infrared correspond to phonons. As temperature is decreased to T_c the reflectance of the most metallic, optimally doped sample increases, while that of the underdoped crystals decreases, due to the formation of the pseudogap.[24–27] At temperatures below T_c the Josephson plasma edge develops, corresponding to coherent oscillation of the nondissipative superconducting condensate. This feature is characterized by very high reflectance at low frequencies followed by a sharp dip at the Josephson plasma resonance (JPR) frequency $\omega_s=\sqrt{\rho_s/\epsilon_\infty}$. This frequency, a direct measure of the superfluid density, softens with oxygen reduction, (from $\omega_{\mathrm{JPR}}=\approx 250\ \mathrm{cm}^{-1}$ at $y=6.95$ to $\omega_{\mathrm{JPR}}=60\ \mathrm{cm}^{-1}$ at $y=6.67$) and stiffens at lower temperatures. Also, in the underdoped crystals a broad, asymmetric feature near 450 cm^{-1} which is weakly visible above T_c becomes significantly more prominent in the superconducting state. These results are consistent with previous studies of similar $YBa_2Cu_3O_y$ compounds.[24,26–31]

Application of magnetic field parallel to the c axis in many respects reverses the trends of lowering temperature. As seen in Fig. 3, for underdoped crystals the field softens the JPR and reduces the magnitude of the asymmetric feature. For $H\| c$ no new features are observed in $R(\omega)$. Magnetic fields $H\| CuO_2$ (Fig. 4), however, do introduce new absorption features at frequencies below the JPR. The frequency of the dip in $R(\omega)$ increases with field, moving from

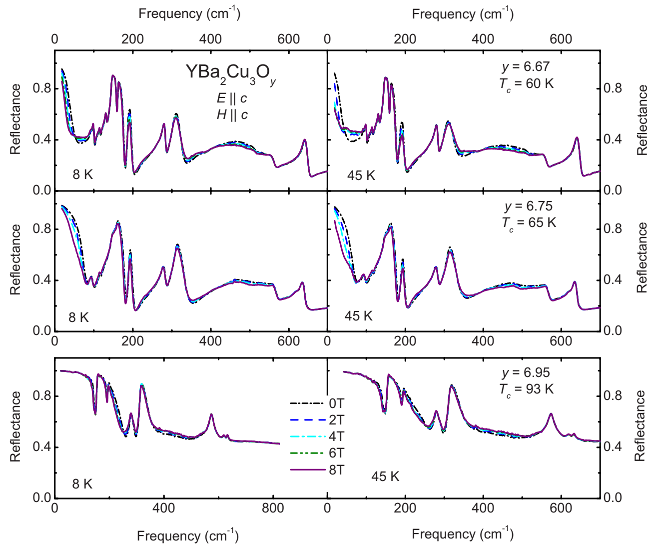

FIG. 3. (Color online) Infrared reflectance $R(\omega)$ of $YBa_2Cu_3O_y$ single crystals for dopings $y=6.67$ (top), 6.75 (middle), and 6.95 (bottom) at temperatures $T=8$ K (left) and 45 K (right). Magnetic fields up to $H=8$ T are applied parallel to the c axis.

26 to 36 cm^{-1} by 8 T. This behavior is consistent with earlier studies of the YBCO system, and has been discussed in detail previously by some of us.[32] The magnetic field $H \| CuO_2$ induces no appreciable changes in the reflectance for frequencies $\omega > 100$ cm^{-1}.

III. OPTICAL CONDUCTIVITY

Reflectance data were transformed via the Kramers-Kronig relations to obtain the optical conductivity $\hat{\sigma}(\omega)$. Because this calculation requires the input of $R(\omega)$ over the full frequency half-space, we augment the raw data with appropriate low- and high-frequency extrapolations. In the normal state we assumed a Hagen-Rubens metallic response of the form $(1-R) \propto \omega^{1/2}$ for frequencies below the lowest measured data. A two-fluid form was assumed in the superconducting state. High frequency data were extended to $+\infty$ with a combination of linear and ω^{-4} asymptotic extrapolations.

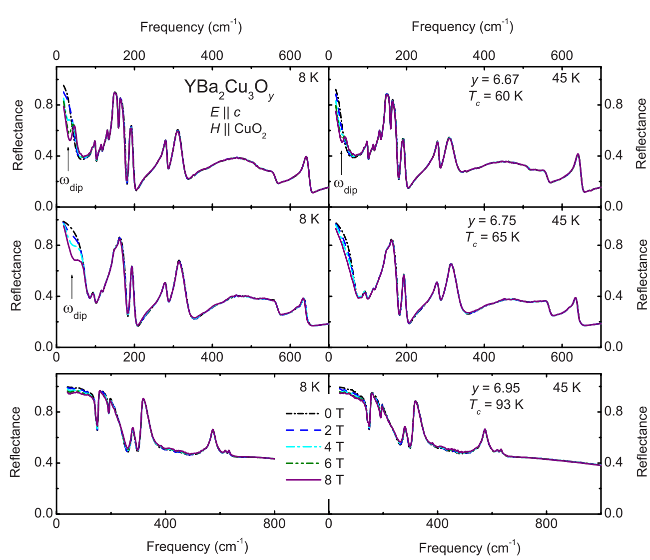

FIG. 4. (Color online) Infrared reflectance $R(\omega)$ of $YBa_2Cu_3O_y$ single crystals for dopings $y=6.67$ (top), 6.75 (middle), and 6.95 (bottom) at temperatures $T=8$ K (left) and 45 K (right). Magnetic fields up to $H=8$ T are applied parallel to the CuO_2 planes.

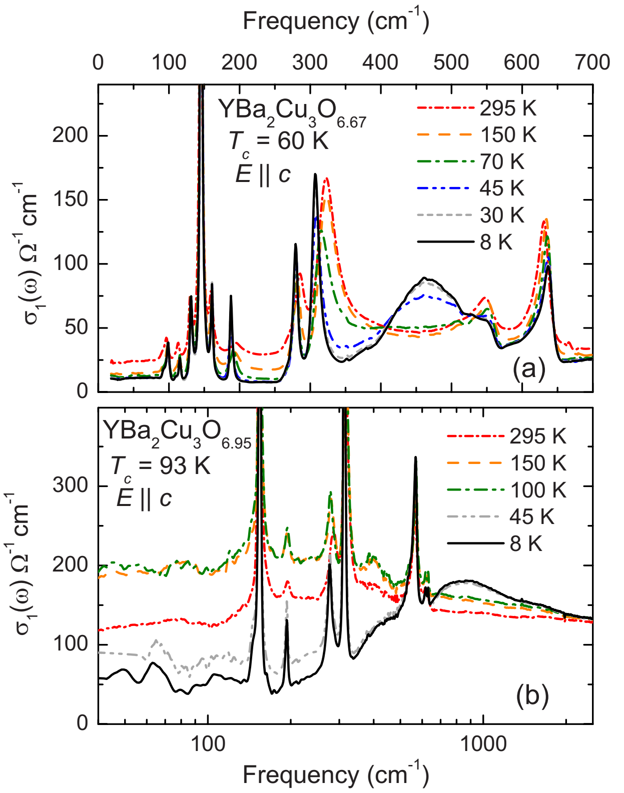

FIG. 5. (Color online) Optical conductivity of $YBa_2Cu_3O_y$ single crystals for dopings (a) $y=6.67$ and (b) 6.95 at several temperatures above and below T_c.

The real part of the optical conductivity $\sigma_1(\omega)$ at zero magnetic field is displayed in Fig. 5. The room temperature conductivity is flat overall, interrupted only by a series of infrared-active phonons. For the optimally doped crystal, the background conductivity increases with decreasing temperature to T_c, consistent with a metallic system. The underdoped crystals, however, become less conductive upon lowering to $T=T_c$, and reach maximum conductivity levels roughly an order of magnitude smaller than those of the optimally doped case. Further cooling reveals a partial gapping of the Fermi surface. characteristic of the pseudogap. In oxygen-reduced crystals spectral weight (SW) is removed from phonons to create a broad band near 450 cm^{-1}. This feature has been previously studied in detail and may be consistent with either a bilayer transverse plasmon mode or a bilayer splitting.[31,33–35]

As found in the reflectance, modifications to the conductivity by the magnetic field are strikingly dissimilar in the different field orientations. For $H \| c$ (Fig. 6) no new modes appear in $\sigma_1(\omega)$, but substantial changes occur in the phonon region. In the underdoped crystals the field initiates a pronounced shift of SW from the asymmetrical mode back into the phonon at 320 cm^{-1}, mirroring the effect of raising tem-

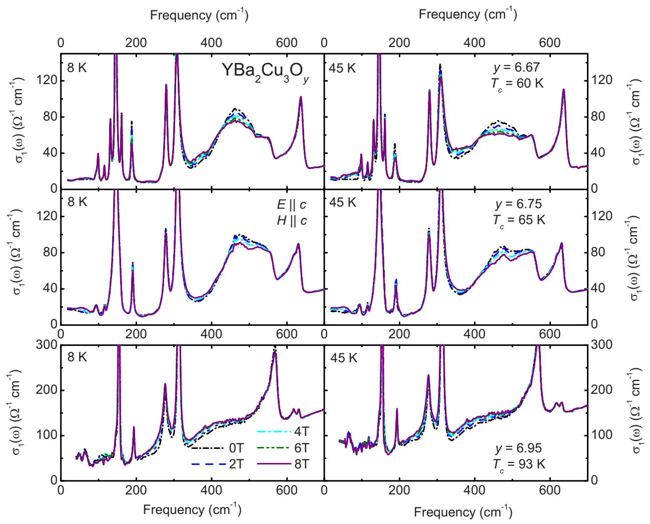

FIG. 6. (Color online) Optical conductivity of $YBa_2Cu_3O_y$ single crystals for dopings $y=6.67$ (top), 6.75 (middle), and 6.95 (bottom) at temperatures $T=8$ K (left) and 45 K (right). Magnetic fields up to $H=8$ T are applied parallel to the c axis.

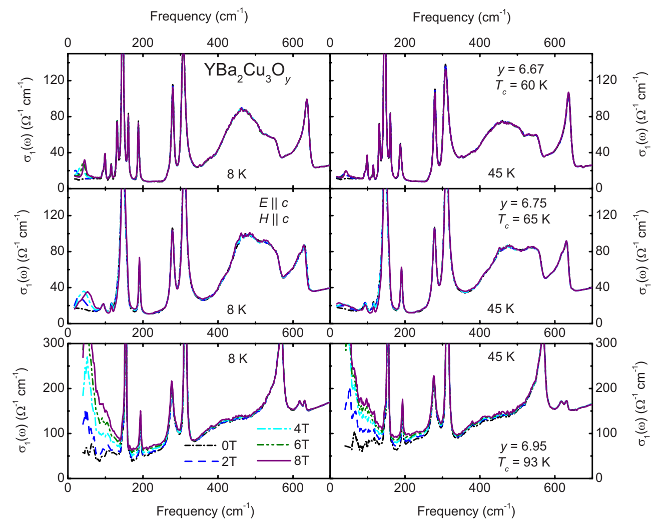

FIG. 8. (Color online) Optical conductivity of $YBa_2Cu_3O_y$ single crystals for dopings $y=6.67$ (top), 6.75 (middle), and 6.95 (bottom) at temperatures $T=8$ K (left) and 45 K (right). Magnetic fields up to $H=8$ T are applied parallel to the CuO_2 planes.

perature. Direct evidence for the equivalence of increasing magnetic field and temperature is found in Fig. 7, where we plot for the $y=6.67$ crystal $\sigma_1(\omega)$ at 8 K (0 and 8 T), 45 K (0 and 8 T) as well as just above T_c at 70 K. Using the 8 K, 0 T result as a starting point, it is clear that both H and T drive the spectrum toward the 70 K curve. The result of raising T to 45 K at zero field is nearly identical to that of raising H to 8 T and keeping T fixed.

The data for fields applied parallel to the CuO_2 planes, shown in Fig. 8, exhibit fundamentally different behavior than was observed for $H \| c$. For magnetic fields $H \| CuO_2$ a resonance appears at low frequencies.[36] With increasing magnetic field the resonance hardens and gains SW. This feature has been shown to have its origin in Josephson vortex lattice dynamics.[32,36,37] Other than minor modifications to the electronic background which affect phonon features, minimal field-induced changes occur at higher frequencies.

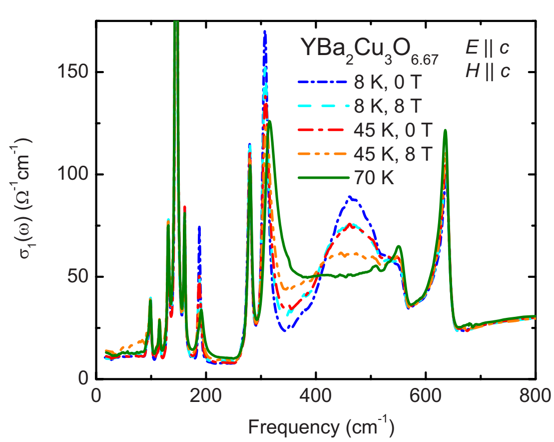

FIG. 7. (Color online) Optical conductivity for $YBa_2Cu_3O_{6.67}$ single crystal at 8 K (0 and 8 T), 45 K (0 and 8 T) and just above T_c at 70 K. Similarity between 8 K, 8 T curve and 45 K, 0 T curve demonstrates equivalence of temperature and magnetic field $H \| c$ for modification of optical properties.

IV. SUM RULES AND SPECTRAL WEIGHT TRANSFER

To investigate in more detail the energy scales governing the superconducting transition we now compare the low-frequency integrated SW with the superfluid density at key values of temperature and magnetic field. We will show that magnetic fields $H \| c$ rapidly eliminate the high-frequency transfer of spectral weight to the superfluid density, while fields $H \| CuO_2$ suppress the high-energy contribution proportionately to the superfluid density. The integral spectral function $\Delta N_{T_c}(\omega,H)=\int_{0^+}^{\omega} d\omega'[\sigma_1(\omega',T_c,0\ \mathrm{T})-\sigma_1(\omega',8\ \mathrm{K},H)]$ quantifies the SW transferred to the $\delta(\omega)$ peak from frequencies less than ω. Representative $\Delta N_{T_c}(\omega,H)$ curves are plotted in Fig. 9 for fields oriented both parallel to the c axis (panels a and b) and to the CuO_2 planes (panels c and d) at $T=8$ K. The values of $\Delta N_{T_c}(\Omega_c)$ are plotted in Figs. 10 and 11 at $T=8$ K (left column) and 45 K (right column) for magnetic fields up to 8 T. Also plotted in Figs. 10 and 11 is the superfluid density $\rho_s(H)$. The zero-frequency superconducting condensate is nondissipative, and thus cannot be directly observed in the $\sigma_1(\omega)$ spectra. Due to causality relations, however, its strength can be deduced from the inductive part of the conductivity $\sigma_2(\omega)$, which behaves as ρ_s/ω in the superconducting state.[38] At each value of magnetic field the difference $\rho_s(H)$-$\Delta N_{T_c}(\omega,H)$ is indicated by the shaded region and labeled as ΔKE to emphasize the connection to the kinetic-energy change, as outlined in Sec. I.

The differing effects of the two magnetic field geometries can be clearly seen in the evolution of low-frequency SW. In general, each $\Delta N_{T_c}(\omega,H)$ spectrum exhibits spikes in the far infrared at frequencies where phonons or other modes are modified. These spikes are superimposed upon a background which increases as a function of frequency through the far infrared, then levels off to a constant value. The cutoff fre-

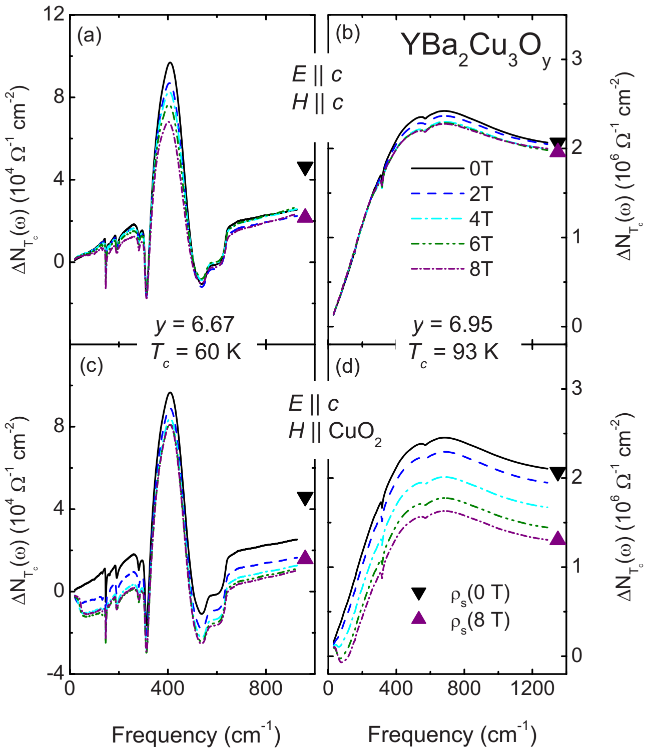

FIG. 9. (Color online) Difference in integrated SW between normal $(T>T_c)$ and superconducting state $\Delta N_{T_c}(\omega,H) = \int_{0^+}^{\omega} d\omega' [\sigma_1(\omega',T_c,0\ \text{T}) - \sigma_1(\omega',8\ \text{K},H)]$ for dopings $y=6.67$ (left) and 6.95 (right). Magnetic fields are applied parallel to the c axis (top) and CuO_2 planes (bottom).

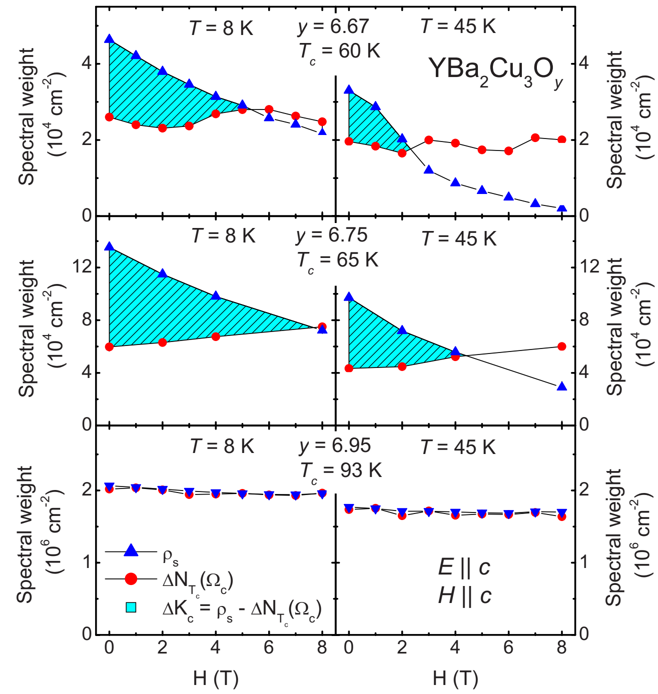

FIG. 10. (Color online) Comparison of spectral weight redistribution in c-axis magnetic field for $YBa_2Cu_3O_y$ at $y=6.67$ (top panel), 6.75 (middle), and 6.95 (bottom) doping levels and temperatures $T=8$ K (left) and 45 K (right). Circles represent the value of $\Delta N_{T_c}(\Omega_c,H)/\rho_s(0\ \text{T})$ at cutoff frequencies $\Omega_c = 1000\ \text{cm}^{-1}$ for the underdoped crystals and $\Omega_c=1300\ \text{cm}^{-1}$ for the optimally doped system. Triangles indicate total superfluid density at each value of magnetic field. High-energy contributions (shaded regions) were inferred from $\rho_s - \Delta N_{T_c}(\Omega_c,H)$ and can be interpreted as kinetic-energy change ΔK_c via Ref. 4.

quencies Ω_c were chosen to be in these flat regions, at $1000\ \text{cm}^{-1}$ for the underdoped crystals and $1300\ \text{cm}^{-1}$ for the optimally doped one. Let us begin with the case of $H \| c$ (top panels). Here, for both underdoped and optimally doped crystals the values of $\Delta N_{T_c}(\omega,H)$ at frequencies above the phonon region are unchanged by magnetic field. The primary impact of magnetic field is simply to redistribute SW within the low-frequency region. Comparing SWs in Fig. 10, we see that for underdoped samples at zero field the value of the superfluid density is nearly twice that of $\Delta N_{T_c}(\omega)$. From this we infer that the extra SW in the superfluid must have been transferred from higher frequencies. As the magnetic field is increased the superfluid density is strongly suppressed, in contrast to the mostly flat behavior of $\Delta N_{T_c}(\Omega_c,H)$. Eventually the two curves cross or merge, with the intersection being driven to lower fields as temperature is increased to 45 K. In the data recorded for the optimally doped crystal, the superfluid density closely matches the missing SW at zero field, and neither quantity is changed by magnetic field.

Application of the magnetic field parallel to the CuO_2 planes results in a qualitatively different picture of SW transfer. For underdoped crystals, the superfluid density behaves similarly to the $H \| c$ orientation, with a strong suppression in field. The low-frequency finite SW change, seen in the bottom panels of Fig. 9, as well as in Fig. 11, is no longer field independent: the limiting values of $\Delta N_{T_c}(\omega,H)$ decrease monotonically with magnetic field, mirroring the $\rho_s(H)$ curve. Thus, the high-frequency SW transfer [the difference between ρ_s and $\Delta N_{T_c}(\Omega_c,H)$] is not entirely suppressed in the superconducting state. Rather, it is gradually diminished, trending toward zero along with the superconducting order parameter. This behavior continues at higher temperatures for the $y=6.75$ crystal. The optimally doped crystal again shows no SW anomaly, with $\Delta N_{T_c}(\omega,H)=\rho_s(H)$ at all fields, even as both are reduced. It should be noted that the field dependence of the magnitudes of the changes for the $y=6.95$ crystal are somewhat extrapolation dependent. However, their equality at all fields holds for any reasonable extrapolation.

The fundamental empirical difference between the results of the two orientations of the magnetic field is the final destination of the SW which is removed from the superfluid density. For $H \| c$ the SW is returned to higher frequencies, thus implying that the energy scale of the condensate formation evolves toward a BCS-like regime. Fields applied $H \| CuO_2$, on the other hand, reduce the high-frequency SW transfer proportionately to the superfluid density, maintaining a discrepancy between $\Delta N_{T_c}(\omega,H)$ and $\rho_s(H)$. This behavior suggests that the mechanism of condensate formation involving transfer of SW from high frequencies remains intact for all values of magnetic field.

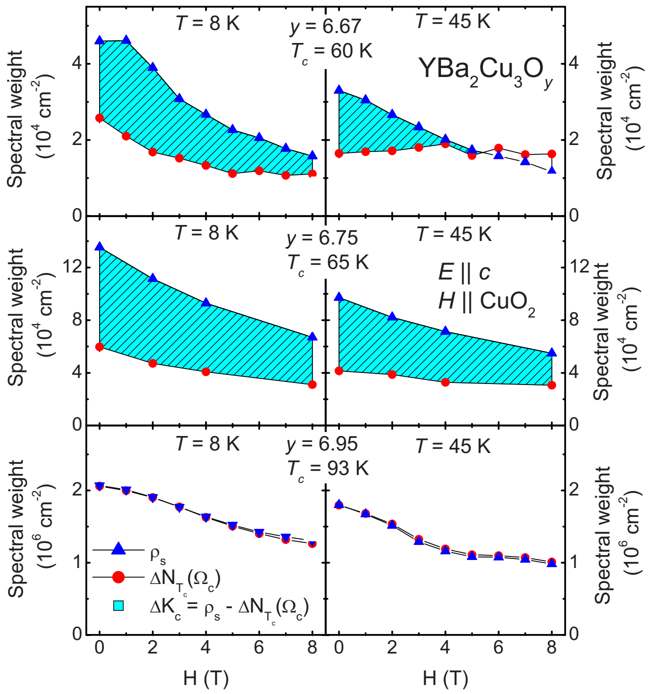

FIG. 11. (Color online) See caption for Fig. 10. Magnetic field is applied parallel to CuO_2 planes.

V. VORTEX MEANDERING AND INTERLAYER PHASE COHERENCE

The dramatic change in the infrared response at relatively small fields $H \| c$ is surprising in several respects. Most notable are the modification of the SW redistribution scheme over an anomalously large energy scale, and the substantial (50%) reduction in superfluid density seen in underdoped samples at fields much smaller than the pair breaking field.[39,40] Both of these effects may be consistent with a theoretical perspective involving the wandering of pancake vortices and the subsequent suppression of interlayer phase coherence.[41,42] In a layered type-II superconductor material with no disorder, it is known that pancake vortices will be well aligned along the *c* axis, maintaining phase coherence between adjacent planes. A disordered pinning potential, however, will produce a random displacement of vortices from layer to layer. As magnetic field is increased this pinning eventually destroys vortex lines and interlayer phase coherence. Since the interlayer phase difference $\phi_{n,n+1}$ is intimately related to the interlayer coupling J and superfluid density ρ_s $[J \propto J_0 \cos(\phi_{n,n+1}) \propto \rho_s]$,[41,42] the effect is visible in the infrared data.

The finite interplane phase difference is central to a model of bilayer dynamics proposed by Ioffe, Millis, and Shah (IMS) in which SW derived from energies far above $k_B T_c$ contributes to ρ_s.[43,44] High-energy SW transfer is expected within the IMS picture when the transition occurs between a normal state above T_c characterized by pairing, but no phase coherence, and a SC state with well-defined phase coherence. One can then extend this description to attribute the elimination of high-energy SW transfer to the competition between vortex meandering and restoration of interlayer phase coherence in magnetic field.

Similar shrinking of the energy scale for condensate formation is not seen in the $H \| CuO_2$ data, consistent with the above considerations of phase coherence. The Josephson vortices created in this field geometry affect the phase of the superconducting order parameter in a more complicated way than pancake vortices do.[37] Oscillations of the Josephson vortex lattice result in an interlayer phase relationship which is dynamic and highly frequency dependent, a departure from the simple linear suppression of coherence expected for pancakes. Furthermore, additional complications arise in the analysis of the IR data obtained in this geometry due to the new resonances in the conductivity spectra which are produced by the motion of Josephson vortices. For vortex-dynamics-related features in $\sigma(\omega)$ the distinction between "normal" and "superconducting" SW is no longer as clear as in the zero-field data. Indeed, these resonances are believed to result from oscillations of Josephson vortices and therefore are of superfluid origin. Yet the features appear in the dissipative part of the conductivity at the expense of the suppression of the superconducting δ peak. Since both the vortex resonance and the Josephson plasma resonance are modified significantly by magnetic field, the SW shifts and possible changes in kinetic energy may be related in a more subtle manner than this analysis allows. Regardless of these complications, the linear scaling of $\Delta N_{T_c}(\Omega_c)$ and ρ_s informs us that high-energy SW transfer is not as easily stifled by $H \| CuO_2$.

Reflectance measurements were also recorded for both magnetic field geometries at temperatures just above the superconducting transition. In both cases no field-induced modifications to the infrared reflectance were observed within the signal to noise of our data. This result has important implications in relation to the subject of preformed pairing. In this theoretical description of the pseudogap, for temperatures between T_c and the pseudogap temperature T^*, Cooper pairs are believed to exist but do not have long-ranged phase coherence.[45,46] The null result above T_c is consistent with the preformed pairs picture since the primary action of magnetic field is to destroy phase coherence, rather than to break Cooper pairs. For this reason, the magnetic field only impacts the optics when phase coherence is appreciable, below T_c. As a result, features in the data which are connected to superconductivity but appear above T_c, such as the asymmetric mode, are not modified by field in this temperature range. It would be highly instructive to extend these measurements to higher magnetic fields to determine if the low-field trends are continued.

It should be noted that the kinetic-energy change observed in *c*-axis polarized experiments is not a phenomenon constrained to the interplane conductivity. In fact, kinetic energy lowering at zero field is consistent with angle-resolved photoemission spectroscopy (ARPES) data measured with *ab*-face crystals (see Ref. 10 and references therein). ARPES measurements of underdoped cuprates at the antinodal $[(\pi,0)$ and $(0,\pi)]$ regions of *k* space reveal indicators of quasiparticle coherence consistent with the IMS picture described above: coherence at temperatures below T_c, but not above.[47,48] Comparison of IR and ARPES data confirms that kinetic-energy change only occurs when this pattern of coherence is observed. Since the *c*-axis electrodynamics are thought to be strongly determined by the properties of the Fermi surface at the antinodal regions, free of the strong nodal contributions inherent to the CuO_2 planes,[49] interplane measurements are especially sensitive to modifications of kinetic energy. In this way, c-axis experiments can be regarded as a probe of superconductivity in the planes.

This study is not unique in its approach of using magnetic field to tune anomalous properties of the high-T_c superconductors. Recent transport measurements[50] of the normal state in overdoped $Tl_2Ba_2CuO_{6+x}$ have shown that magnetic field $H \| c$ can tune the ground state from non-Fermi liquid to Fermi liquid in the vicinity of a quantum critical point. This strong modification of the electronic structure by magnetic field points toward the important role which spin plays in this doped Mott insulator system, even far from the antiferromagnetic region of the phase diagram. Other interesting connections between spin and electromagnetic response were uncovered by magneto-optical studies[51] of $La_{2-x}Sr_xCuO_4$ in which c-axis magnetic fields were shown to promote antiferromagnetism in the CuO_2 planes.

VI. CONCLUSION

The primary finding of this work is that the application of an external magnetic can initiate profound redistribution of spectral weight from the superfluid density to the finite-frequency spectrum. The character of these effects differs depending on the orientation of the field with respect to the CuO_2 planes. Fields $H \| c$ return weight to high-energy regions of the spectrum, undoing the lowering of kinetic energy observed at zero field. Fields $H \| CuO_2$ place the weight at frequencies on the order of the superconducting gap, maintaining the reduction in kinetic energy. Since it is possible to reduce the interlayer phase coherence to the point where high-energy spectral weight transfer ceases, but a robust superconducting state remains, we must conclude that the reduction in kinetic energy seen at zero field is not a necessary condition for superconductivity. The importance of the phase coherence to this process is supported by the data for fields $H \| CuO_2$; these fields are less destructive to the interlayer phase relationship and leave intact the kinetic-energy reduction intact.

ACKNOWLEDGMENTS

This research was supported by NSF Grant No. DMR 0705171. Y.A. was supported by KAKENHI Grants No. 19674002 and No. 20030004, as was K.S. by KAKENHI Grant No. 20740196.

*alaforge@physics.ucsd.edu

†Present address: Department of Physics, Boston College, 140 Commonwealth Ave., Chestnut Hill, MA 02467, USA.

‡Present address: Department of Physics, University of Toronto, Toronto, Ontario, M5S 1A7 Canada.

[1] R. Kubo, J. Phys. Soc. Jpn. **12**, 570 (1957).

[2] P. F. Maldague, Phys. Rev. B **16**, 2437 (1977).

[3] D. Baeriswyl, C. Gros, and T. M. Rice, Phys. Rev. B **35**, 8391 (1987).

[4] J. E. Hirsch, Physica C **199**, 305 (1992).

[5] S. Chakravarty, Hae-Young Kee, and E. Abrahams, Phys. Rev. Lett. **82**, 2366 (1999).

[6] D. N. Basov and T. Timusk, Rev. Mod. Phys. **77**, 721 (2005).

[7] R. A. Ferrell and R. E. Glover III, Phys. Rev. **109**, 1398 (1958).

[8] For a theoretical perspective, see, for example, A. J. Leggett, Nat. Phys. **2**, 134 (2006).

[9] D. N. Basov, S. I. Woods, A. S. Katz, E. J. Singley, R. C. Dynes, M. Xu, D. G. Hinks, C. C. Homes, and M. Strongin, Science **283**, 49 (1999).

[10] D. N. Basov, C. C. Homes, E. J. Singley, M. Strongin, T. Timusk, G. Blumberg, and D. van der Marel, Phys. Rev. B **63**, 134514 (2001).

[11] A. S. Katz, S. I. Woods, E. J. Singley, T. W. Li, M. Xu, D. G. Hinks, R. C. Dynes, and D. N. Basov, Phys. Rev. B **61**, 5930 (2000).

[12] H. J. A. Molegraaf, C. Presura, D. van der Marel, P. H. Kes, and M. Li, Science **295**, 2239 (2002).

[13] A. B. Kuzmenko, N. Tombros, H. J. A. Molegraaf, M. Gruninger, D. van der Marel, and S. Uchida, Phys. Rev. Lett. **91**, 037004 (2003).

[14] C. C. Homes, S. V. Dordevic, D. A. Bonn, R. Liang, and W. N. Hardy, Phys. Rev. B **69**, 024514 (2004).

[15] A. F. Santander-Syro, R. P. S. M. Lobo, N. Bontemps, W. Lopera, D. Girata, Z. Konstantinovic, Z. Z. Li, and H. Raffy, Phys. Rev. B **70**, 134504 (2004).

[16] A. V. Boris, N. N. Kovaleva, O. V. Dolgov, T. Holden, C. T. Lin, B. Keimer, and C. Bernhard, Science **304**, 708 (2004).

[17] Li Yu, D. Munzar, A. V. Boris, P. Yordanov, J. Chaloupka, Th. Wolf, C. T. Lin, B. Keimer, and C. Bernhard, Phys. Rev. Lett. **100**, 177004 (2008).

[18] For connection to other spectroscopic results, see, for example, M. R. Norman, M. Randeria, B. Janko, and J. C. Campuzano, Phys. Rev. B **61**, 14742 (2000).

[19] A. D. LaForge, W. J. Padilla, K. S. Burch, Z. Q. Li, A. A. Schafgans, Kouji Segawa, Yoichi Ando, and D. N. Basov, Phys. Rev. Lett. **101**, 097008 (2008).

[20] X. F. Sun, Kouji Segawa, and Yoichi Ando, Phys. Rev. Lett. **93**, 107001 (2004).

[21] Kouji Segawa and Yoichi Ando, Phys. Rev. B **69**, 104521 (2004).

[22] C. C. Homes, M. Reedyk, D. A. Cradles, and T. Timusk, Appl. Opt. **32**, 2976 (1993).

[23] W. J. Padilla, Z. Q. Li, K. S. Burch, Y. S. Lee, K. J. Mikolaitis, and D. N. Basov, Rev. Sci. Instrum. **75**, 4710 (2004).

[24] C. C. Homes, T. Timusk, R. Liang, D. A. Bonn, and W. N. Hardy, Phys. Rev. Lett. **71**, 1645 (1993).

[25] D. N. Basov, T. Timusk, B. Dabrowski, and J. D. Jorgensen, Phys. Rev. B **50**, 3511 (1994).

[26] C. C. Homes, T. Timusk, D. A. Bonn, R. Liang, and W. N. Hardy, Physica C **254**, 265 (1995).

[27] C. Bernhard, D. Munzar, A. Wittlin, W. Konig, A. Golnik, C. T. Lin, M. Kläser, Th. Wolf, G. Müller-Vogt, and M. Cardona, Phys. Rev. B **59**, R6631 (1999).
[28] D. N. Basov, H. A. Mook, B. Dabrowski, and T. Timusk, Phys. Rev. B **52**, R13141 (1995).
[29] J. Schützmann, S. Tajima, S. Miyamoto, Y. Sato, and R. Hauff, Phys. Rev. B **52**, 13665 (1995).
[30] S. Tajima, J. Schutzmann, S. Miyamoto, I. Terasaki, Y. Sato, and R. Hauff, Phys. Rev. B **55**, 6051 (1997).
[31] C. Bernhard, D. Munzar, A. Golnik, C. T. Lin, A. Wittlin, J. Humlicek, and M. Cardona, Phys. Rev. B **61**, 618 (2000).
[32] A. D. LaForge, W. J. Padilla, K. S. Burch, Z. Q. Li, S. V. Dordevic, Kouji Segawa, Yoichi Ando, and D. N. Basov, Phys. Rev. B **76**, 054524 (2007).
[33] D. Munzar, C. Bernhard, A. Golnik, J. Humlìcek, and M. Cardona, Solid State Commun. **112**, 365 (1999).
[34] M. Gruninger, D. van der Marel, A. A. Tsvetkov, and A. Erb, Phys. Rev. Lett. **84**, 1575 (2000).
[35] S. V. Dordevic, E. J. Singley, J. H. Kim, M. B. Maple, S. Komiya, S. Ono, Y. Ando, T. Rõõm, R. Liang, D. A. Bonn, W. N. Hardy, J. P. Carbotte, C. C. Homes, M. Strongin, and D. N. Basov, Phys. Rev. B **69**, 094511 (2004).
[36] K. M. Kojima, S. Uchida, Y. Fudamoto, and S. Tajima, Phys. Rev. Lett. **89**, 247001 (2002).
[37] A. E. Koshelev, Phys. Rev. B **76**, 054525 (2007).
[38] S. V. Dordevic, E. J. Singley, and D. N. Basov, Seiki Komiya, Yoichi Ando, E. Bucher, C. C. Homes, and M. Strongin, Phys. Rev. B **65**, 134511 (2002).
[39] Y. Ando and K. Segawa, Phys. Rev. Lett. **88**, 167005 (2002).
[40] Y. S. Lee, Kouji Segawa, Z. Q. Li, W. J. Padilla, M. Dumm, S. V. Dordevic, C. C. Homes, Yoichi Ando, and D. N. Basov, Phys. Rev. B **72**, 054529 (2005).
[41] A. E. Koshelev, L. I. Glazman, and A. I. Larkin, Phys. Rev. B **53**, 2786 (1996).
[42] L. N. Bulaevskii, A. E. Koshelev, V. M. Vinokur, and M. P. Maley, Phys. Rev. B **61**, R3819 (2000).
[43] L. B. Ioffe and A. J. Millis, Science **285**, 1241 (1999).
[44] N. Shah and A. J. Millis, Phys. Rev. B **65**, 024506 (2001).
[45] V. J. Emery and S. A. Kivelson, Nature (London) **374**, 434 (1995).
[46] J. Corson, R. Mallozzi, J. Orenstein, J. N. Eckstein, and I. Bozovic, Nature (London) **398**, 221 (1999).
[47] H. Ding, T. Yokoya, J. C. Campuzano, T. Takahashi, M. Randeria, M. R. Norman, T. Mochiku, K. Kadowaki, and J. Giapintzakis, Nature (London) **382**, 51 (1996).
[48] A. G. Loeser, Z.-X. Shen, D. S. Dessau, D. S. Marshall, C. H. Park, P. Fournier, and A. Kapitulnik, Science **273**, 325 (1996).
[49] S. Chakravarty, A. Sudbo, P. W. Andersen, and S. Strong, Science **261**, 337 (1993).
[50] T. Shibauchi, L. Krusin-Elbaum, M. Hasegawa, Y. Kasahara, R. Okazaki, and Y. Matsuda, Proc. Natl. Acad. Sci. U.S.A. **105**, 7120 (2008).
[51] A. A. Schafgans, A. D. LaForge, S. V. Dordevic, and M. M. Qazilbash, Seiki Komiya, Yoichi Ando, and D. N. Basov (unpublished).